PAPER

New insight into the crystal structure of Sr$_4$Ca(PO$_4$)$_2$SiO$_4$ and the photoluminescence tuning of Sr$_4$Ca(PO$_4$)$_2$SiO$_4$:Ce^{3+},Na$^+$,Eu^{2+} phosphors†

Manli Zhang,[a] Zhiguo Xia,*[a] Maxim S. Molokeev,[bc] Lin Shi[a] and Quanlin Liu[a]

A new single phase based on the substitution of a Sr cation by a Ca cation in the apatite-type Sr$_5$(PO$_4$)$_2$(SiO$_4$) has been fabricated with the nominal chemical composition of Sr$_4$Ca(PO$_4$)$_2$(SiO$_4$), which appears as a definite compound rather than a solid solution between (Sr,Ca)$_3$(PO$_4$)$_2$ and (Sr,Ca)$_2$SiO$_4$. The crystal structure of Sr$_4$Ca(PO$_4$)$_2$(SiO$_4$) has been firstly analysed by the difference electron map, and further resolved by the Rietveld refinement, and the final composition has been determined as Sr$_4$Ca(PO$_4$)$_{(2+x)}$(SiO$_4$)$_{(1-x)}$(OH)$_x$ (x = 0.64) with a hexagonal cell (P6$_3$/m). The Ce^{3+}/Eu^{2+} codoped Sr$_4$Ca(PO$_4$)$_2$SiO$_4$ phosphors have been designed and prepared by the solid state method, and the photoluminescence tuning from blue to green upon 365 nm ultraviolet (UV) radiation can be realized, which is ascribed to the energy transfer from Ce^{3+} to Eu^{2+} ions. The luminescence properties and the energy transfer mechanism in Ce^{3+}/Eu^{2+} codoped Sr$_4$Ca(PO$_4$)$_2$SiO$_4$ phosphors have been discussed, which might act as potential candidates for blue-green components in UV-pumped white light emitting diodes (WLEDs).

1. Introduction

Apatite minerals form a large family of inorganic compounds with the general formula of M$_{10}$(TO$_4$)$_6$X$_2$ (M = Ca^{2+}, Sr^{2+}, Ba^{2+}; TO$_4$ = PO$_4$$^{3-}$, VO$_4$$^{3-}$, AsO$_4$$^{3-}$; X = OH$^-$, F$^-$, Cl$^-$), which crystallize in a hexagonal system (space group P6$_3$/m) and the structures are characterized by the presence of tunnels containing mobile X ions.[1–3] In recent years, apatite-like compounds have been widely investigated for many kinds of applications including biocompatible materials, electrolytes, phosphor hosts for white light emitting diodes (WLEDs), and so on.[4–6] As an adaptable crystal structure, the newly reported concept on the chemical unit cosubstitution can be used to design new apatite-type compounds or some derived phases.[7–9] Accordingly, compared to the typical apatite compound (Sr,Ca)$_5$(TO$_4$)$_3$X, the (Sr,Ca)$_5$(PO$_4$)$_2$(SiO$_4$) phase was designed from the substitution of (PO$_4$)$^{3-}$ + X$^-$ → (SiO$_4$)$^{4-}$, and there does not exist any halogen atoms in the structure. However, the crystal structure of (Sr,Ca)$_5$(PO$_4$)$_2$(SiO$_4$) has some

relationship to that of the apatite phase but not isotypic.[10] In some cases, it can also be related to the solid solution between (Sr,Ca)$_3$(PO$_4$)$_2$ and (Sr,Ca)$_2$SiO$_4$, but they are totally different upon checking their corresponding crystallographic parameters. Nevertheless, we know that both β-Ca$_3$(PO$_4$)$_2$ type (Sr,Ca)$_3$(PO$_4$)$_2$ and orthosilicate phase (Sr,Ca)$_2$SiO$_4$ belong to the excellent phosphor host, and Eu^{2+}/Ce^{3+} in these hosts can show excellent luminescence properties with broad-band excitation and emission, tunable emission from blue to red, and high luminescence efficiencies, and so on.[11–13]

Therefore, the excellent luminescence properties of Eu^{2+}/Ce^{3+} in the (Sr,Ca)$_5$(PO$_4$)$_2$(SiO$_4$) phase and potential diverse applications are also expected.[14] Previously, Blasse briefly reported the luminescence of Eu^{2+} in Sr$_5$(PO$_4$)$_2$(SiO$_4$);[15] after that, Seo's and Hong's group reported the green-emitting Sr$_5$(PO$_4$)$_2$(SiO$_4$):Eu^{2+} and Ca$_5$(PO$_4$)$_2$-(SiO$_4$):Eu^{2+} phosphors for WLEDs, respectively.[16,17] Moreover, Seo's group reported the structural phase formation and tunable luminescence in (Ca,Sr,Ba)$_5$(PO$_4$)$_2$(SiO$_4$):Eu^{2+} phosphors;[18] Wang's group reported the white light emitting mono Ce^{3+} doped Sr$_5$(PO$_4$)$_2$-(SiO$_4$) phosphors;[19] and Lin's group reported the tunable luminescence and energy transfer properties of single-composition phosphors Ca$_5$(PO$_4$)$_2$(SiO$_4$):Ce^{3+},Tb^{3+},Mn^{2+}.[20] It is clearly found that Eu^{2+}/Ce^{3+} doped (Sr,Ca)$_5$(PO$_4$)$_2$(SiO$_4$) phosphors demonstrated interesting luminescence properties and deserved extensive investigations. However, we can also find that the intermediate compositions in such a kind of compounds have no report, and the crystal structure of the (Sr,Ca)$_5$(PO$_4$)$_2$(SiO$_4$) phase is not well established.

^{a} School of Materials Sciences and Engineering, University of Science and Technology Beijing, Beijing 100083, China. E-mail: xiazg@ustb.edu.cn; Fax: +86-10-8237-7955; Tel: +86-10-8237-7955

^{b} Laboratory of Crystal Physics, Kirensky Institute of Physics, SB RAS, Krasnoyarsk 660036, Russia

^{c} Department of Physics, Far Eastern State Transport University, Khabarovsk 680021, Russia

† Electronic supplementary information (ESI) available. See DOI: 10.1039/c6tc03373c

9078 | *J. Mater. Chem. C*, 2016, **4**, 9078–9084

This journal is © The Royal Society of Chemistry 2016

In the present study, a new single phase based on the substitution of a Sr cation by a Ca cation in $Sr_5(PO_4)_2(SiO_4)$ has been prepared with the nominal chemical composition of $Sr_4Ca(PO_4)_2(SiO_4)$. On the basis of the difference electron map and Rietveld refinement from the XRD pattern, the final composition of $Sr_4Ca(PO_4)_2(SiO_4)$ has been determined as $Sr_4Ca(PO_4)_{(2+x)}(SiO_4)_{(1-x)}(OH)_x$ ($x = 0.64$) with a hexagonal cell ($P6_3/m$), and the crystal structure has been carefully described in this paper. Moreover, Ce^{3+}/Eu^{2+} codoped $Sr_4Ca(PO_4)_2SiO_4$ phosphors have been prepared by the solid state method, and the photoluminescence tuning from blue to green has been realized based on the energy transfer of Ce^{3+} to Eu^{2+} ions, which might act as potential candidates for blue-green components in UV-pumped WLEDs.

2. Experimental section

2.1 Materials and synthesis

The nominal $Sr_4Ca(PO_4)_2(SiO_4)$ compound and the phosphors of $Sr_{3.8-x}Ca(PO_4)_2SiO_4:0.1Ce^{3+},0.1Na^+,xEu^{2+}$ ($x = 0$, 0.003, 0.01, 0.03 and 0.06) were prepared by the conventional solid-state reaction method. The starting materials were $SrCO_3$ (99.99%), $CaCO_3$ (99.99%), $NH_4H_2PO_4$ (99.99%), SiO_2 (99.99%), Na_2CO_3 (99.99%), CeO_2 (99.99%) and Eu_2O_3 (99.99%). Among them, the monovalent cation Na^+ is used to realize charge equalization when the trivalent activator Ce^{3+} was used to replace the Sr^{2+} ions. The stoichiometric chemicals were weighed as the above nominal compositions and thoroughly mixed in an agate mortar, then transferred to a corundum crucible and heated at 1400 °C (in reductive atmosphere) for 6 h. Finally, the prepared phosphors were cooled to room temperature and reground for further measurements.

2.2 Characterization

The phase structures of the as-synthesized samples were checked using a D8 Advance diffractometer (Bruker Corporation, Germany) operating at 40 kV and 40 mA under Cu Kα radiation ($\lambda = 1.5406$ Å). The photoluminescence emission (PL) and photoluminescence excitation (PLE) spectra were recorded using a fluorescence spectrophotometer (F-4600, HITACHI, Japan) equipped with a photomultiplier tube operating at 400 V, and a 150 W Xenon lamp as the excitation source. The temperature dependent photoluminescence spectra have been measured by the same spectrophotometer, and it was combined with a self-made heating attachment and a computer-controlled electric furnace (Tianjin Orient KOJI Co., Ltd, TAP-02). The luminescence decay curves were obtained using a FLSP9200 fluorescence spectrophotometer (Edinburgh Instruments Ltd, UK), and an nF900 flash lamp was used as the excitation source.

3. Results and discussion

3.1 Phase formation and crystal structure

The diffraction data of the as-prepared nominal $Sr_4Ca(PO_4)_2(SiO_4)$ compound for Rietveld analysis were collected at room temperature with a step size of 2θ being 0.01313°, and the counting time was 5 s per step. Rietveld refinement was performed by using TOPAS 4.2. Almost all peaks were indexed to the hexagonal cell ($P6_3/m$) with parameters close to $Sr_5(PO_4)_3(OH)$ (strontium-apatite structure).[21] Therefore, the crystal structure of $Sr_5(PO_4)_3(OH)$ was taken as a starting model for Rietveld refinement. Sites of Sr ions were equally occupied by Sr and Ca ions, the site of P was also occupied by P and Si randomly. All these occupancies were refined in an assumption that the sum of occupancies in each site is equal to 1. The OH group was deleted at the first stage of refinement due to the suggested formula $Sr_4Ca(PO_4)_2SiO_4$. Refinement gave a low R-factor ($R_B = 1.99\%$). However, as given in Fig. 1, it demonstrated the difference electron map calculated using the $F_{obs} - F_{calc}$ difference of observed and calculated structural amplitudes (herein, F_{obs} are the observed structure-factor amplitudes, F_{calc} are the calculated structure-factor amplitudes which were calculated from the atom coordinates of the model). The results showed maxima at $(0, 0, x)$ ($x \sim 0.2$) and several symmetry equivalent maxima. It was known that these peaks corresponded to OH^- ions because $(0, 0, 0.2)$ is close to the position of the OH^- ion $(0, 0, 0.1856(14))$ in $Sr_5(PO_4)_3(OH)$. Therefore it was suggested to return the OH group in the model. It is believed that the residual H_2O molecules combined with starting materials and the H_2O in the air can promote the phase formation of $Sr_4Ca(PO_4)_{(2+x)}(SiO_4)_{(1-x)}(OH)_x$, which enabled the presence of the OH^- group. According to this observation and the difference electron map analysis in Fig. 1, the chemical formula should be rewritten as $Sr_4Ca(PO_4)_{(2+x)}(SiO_4)_{(1-x)}(OH)_x$ in order to keep the sum of charges to be zero. On the basis of such a model, Fig. 2 gives the Rietveld analysis patterns for X-ray powder diffraction data of the nominal $Sr_4Ca(PO_4)_2(SiO_4)$ compound, and the value of x was determined; the final refinement was stable and gave low R-factors (Table 1 and Fig. 2), and the R_B factor dropped to 1.93%. The inset in Fig. 2 shows the representative crystal structure of $Sr_4Ca(PO_4)_{(2+x)}(SiO_4)_{(1-x)}(OH)_x$, which crystallized in the hexagonal cell (space group $P6_3/m$) with lattice constants $a = b = 9.67202$ (8), $c = 7.25393$ (7), $V = 587.68$ (1), $Z = 2$, as shown in Table 1, and the crystallographic information file (CIF) is presented in the ESI.†
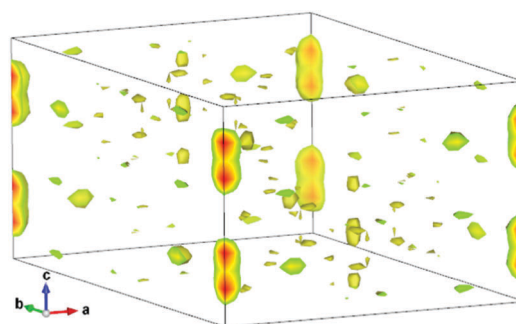

Fig. 1 Difference electron map calculated using the $F_{obs} - F_{calc}$ difference of structural amplitudes for the as-prepared nominal $Sr_4Ca(PO_4)_2SiO_4$ phase with the real composition of $Sr_4Ca(PO_4)_{(2+x)}(SiO_4)_{(1-x)}(OH)_x$. Maxima at $(0, 0, x)$ ($x \sim 0.2$) correspond to missed O ions.
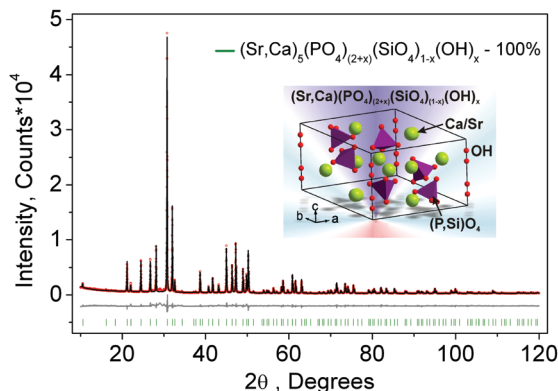
Fig. 2 Rietveld analysis patterns for X-ray powder diffraction data of the nominal $Sr_4Ca(PO_4)_2(SiO_4)$ compound. The solid black lines are calculated intensities, and the red dots are the observed intensities. The gray solid lines below the profiles stand for the difference between the observed and calculated intensities. The short green vertical lines show the position of the Bragg reflections of the calculated pattern. The final chemical formula was refined as $Sr_4Ca(PO_4)_{(2+x)}(SiO_4)_{(1-x)}(OH)_x$, $x = 0.64(3)$ for the as-prepared nominal $Sr_4Ca(PO_4)_2SiO_4$ phase. The inset shows the representative crystal structure of $Sr_4Ca(PO_4)_{(2+x)}(SiO_4)_{(1-x)}(OH)_x$.

Table 1 Main parameters of processing and refinement of the $Sr_4Ca(PO_4)_{(2+x)}(SiO_4)_{(1-x)}(OH)_x$ phase

Phase	$Sr_4Ca(PO_4)_{(2+x)}(SiO_4)_{(1-x)}(OH)_x$ ($x = 0.64(3)$)
Weight, %	100
Sp.Gr.	$P6_3/m$
a, Å	9.67202 (8)
b, Å	9.67202 (8)
c, Å	7.25393 (7)
V, Å³	587.68 (1)
Z	2
2θ-interval, °	10–120
R_{wp}, %	8.46
R_p, %	5.97
R_{exp}, %	3.86
χ^2	2.19
R_B, %	1.93

We have also checked the phase purity of the as-prepared Ce^{3+}/Eu^{2+} codoped $Sr_4Ca(PO_4)_2SiO_4$ phosphors. Fig. 3 shows the representative XRD patterns of $Sr_{3.8−x}Ca(PO_4)_2SiO_4$:$0.1Ce^{3+}$,$0.1Na^+$,$xEu^{2+}$ (x = 0, 0.03) samples. Firstly, the diffraction peaks agree well with the phase of $Sr_4Ca(PO_4)_{(2+x)}(SiO_4)_{(1-x)}(OH)_x$, x = 0.64(3) refined by the Rietveld analysis, as shown in Fig. 2. Secondly, it is obvious that all the diffraction peaks of these samples can also be indexed to the pure hexagonal phase of $Sr_5(PO_4)_2SiO_4$ (JCPDS 21-1187). No other phase is detected after doping, indicating that Ce^{3+} or Eu^{2+} ions were completely dissolved in the nominal $Sr_4Ca(PO_4)_2SiO_4$ host without leading to any significant changes in the crystal structure. However, as discussed above, $Sr_4Ca(PO_4)_{(2+x)}(SiO_4)_{(1-x)}(OH)_x$ and title phase $Sr_4Ca(PO_4)_2SiO_4$ are isostructural. Only one difference – the presence or absence of OH groups in the void of the structure can be found. The X-ray diffraction method is an effective approach to check the presence of OH groups using difference electron density maps mentioned above. It is clear that the addition of some amount of $OH^−$ ions to the structure enables
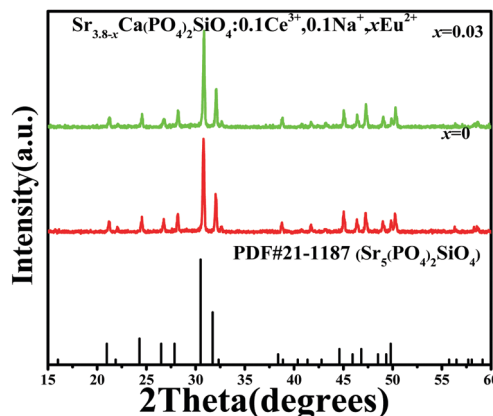

Fig. 3 XRD patterns of as-prepared $Sr_{3.8−x}Ca(PO_4)_2SiO_4$:$0.1Ce^{3+}$,$0.1Na^+$,$xEu^{2+}$ (x = 0, 0.03) samples. The standard data for $Sr_5(PO_4)_2SiO_4$(PDF#21-1187) are shown as the reference.

charge imbalance. In order to make the charge of unit cell equal to zero the following mechanism was suggested: $OH^− + PO_4^{3−} = SiO_4^{4−}$. Therefore the chemical formula of such compounds should be $Sr_4Ca(PO_4)_{(2+x)}(SiO_4)_{(1-x)}(OH)_x$. Therefore, we still used the chemical formula of the nominal $Sr_4Ca(PO_4)_2SiO_4$ phase in the following section in order to discuss the photoluminescence properties of Ce^{3+}/Eu^{2+} codoped samples.

3.2 Luminescence properties of Ce^{3+}/Na^+ singly doped $Sr_4Ca(PO_4)_2SiO_4$ phosphors

In order to investigate the luminescence properties of Ce^{3+} activated $Sr_4Ca(PO_4)_2SiO_4$ phosphors, we firstly prepared a series of samples $Sr_{3.8−2x}Ca(PO_4)_2SiO_4$:$xCe^{3+}$,$xNa^+$ (x = 0.01, 0.03, 0.05, 0.07, 0.10 and 0.15). Fig. 4a depicts the PLE and PL spectra of the selected $Sr_{3.8}Ca(PO_4)_2SiO_4$:$0.1Ce^{3+}$,$0.1Na^+$ phosphor. The PLE spectrum monitored at 428 nm exhibits a broad band from 250 to 400 nm, which is ascribed to the transitions from the ground state of the Ce^{3+} ions to the field splitting levels of the 5d state.[22] The PL spectrum consists of an asymmetric broad band peaking at 428 nm under the excitation of 365 nm. As we know, such an asymmetric broad band should be ascribed to the characteristics of double band emission of Ce^{3+}, which is due to the transition of Ce^{3+} ions from the 5d excited state to the $^2F_{7/2}$ and $^2F_{5/2}$ ground states. Fig. 4b shows the PL spectra of $Sr_{3.8−2x}Ca(PO_4)_2SiO_4$:$xCe^{3+}$,$xNa^+$ depending on different Ce^{3+} doping content x. All the PL spectra exhibited a similar broad band emission centered at 428 nm, which was also ascribed to the $5d^1$–$4f^1$ of Ce^{3+} ions. The optimal Ce^{3+} dopant content was found to be 0.1 mol per formula unit and the PL intensity was observed to increase with increasing x when $x < 0.1$. That is to say, with the Ce^{3+} dopant content being higher than 0.1, concentration quenching was observed and the PL intensity was found to decrease with increasing Ce^{3+}.

Accordingly, the inset of Fig. 5 presents the PL emission intensities as a function of Ce^{3+} content for $Sr_{3.8−2x}Ca(PO_4)_2SiO_4$:$xCe^{3+}$,$xNa^+$, and it is obvious that the optimal doping concentration is x = 0.1 and then decreased, resulting from the concentration quenching effect. It is known that the
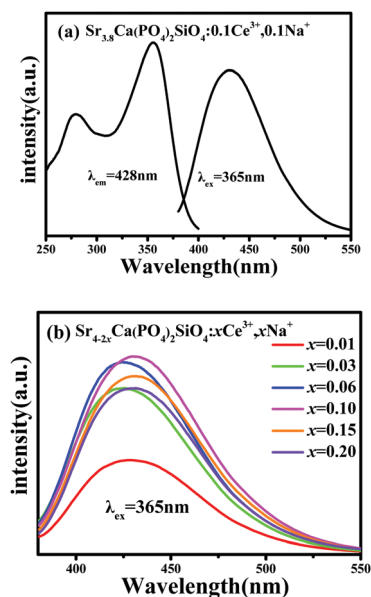
Fig. 4 (a) PLE and PL spectra of $Sr_{3.8}Ca(PO_4)_2SiO_4$:$0.1Ce^{3+}$,$0.1Na^+$, (b) PL spectra of $Sr_{3.8-2x}Ca(PO_4)_2SiO_4$:$xCe^{3+}$,$xNa^+$ (x = 0.01, 0.03, 0.06, 0.10, 0.15 and 0.20).

interaction type between sensitizers or between the sensitizer and the activator can be calculated using the following eqn (1) and it can be used to predict the mechanism of energy transfer and enable concentration quenching. Therefore, we can get the detailed information of multipolar interaction from the variation of the emission intensity depending on the concentration of the activators according to the report of Van Uitert. The emission intensity (I) per activator concentration (x) follows the following equation:[23]

$$\frac{I}{x} = K\left[1 + \beta(x)^{\theta/3}\right]^{-1} \quad (1)$$

where I is the emission intensity, x is the concentration of the activator ions above the concentration quenching point, β and K are constants under the same conditions, and θ is the function of multipole–multipole interaction. When the value of θ is 6, 8 or 10, the form of the interaction corresponds to dipole–dipole (d–d), dipole–quadrupole (d–q), or quadrupole–quadrupole
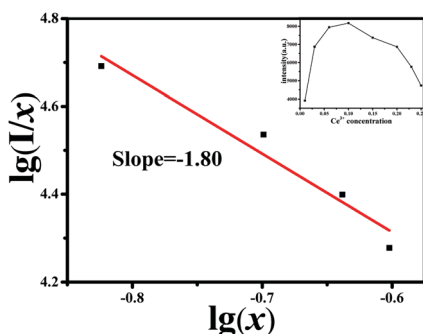
(q–q), respectively. To obtain a correct θ, the dependence of $\lg(I/x)$ on $\lg(x)$ is plotted, and it yields a straight line with a slope of $-\theta/3$. The fitting result for Ce^{3+} emission centers, which is corresponding to the $Sr_{3.8-2x}Ca(PO_4)_2SiO_4$:$xCe^{3+}$,$xNa^+$ phosphor compositions beyond the quenching concentration of Ce^{3+}, is shown in Fig. 5. The slope is determined to be -1.80, through which the value of y can be calculated as 5.4. Therefore, the values are approximately equal to 6, which means that the quenching process is ascribed to the dipole–dipole interaction in the present system.[24,25]

3.3 Luminescence properties and energy transfer of $Sr_4Ca(PO_4)_2SiO_4$:Ce^{3+},Na^+,Eu^{2+} phosphors

As discussed above, the $Sr_4Ca(PO_4)_2SiO_4$ phase belongs to a kind of versatile host for the activators. Therefore, Fig. 4 comparatively demonstrated the emission and excitation spectra of Ce^{3+}/Na^+ and Eu^{2+} singly doped and Ce^{3+}/Na^+/Eu^{2+}-co-doped $Sr_4Ca(PO_4)_2SiO_4$ phosphors. Fig. 6a displays the PL and PLE spectra of the $Sr_{3.8}Ca(PO_4)_2SiO_4$:$0.1Ce^{3+}$,$0.1Na^+$ phosphor. The broad-band emission and excitation spectral characteristics have been discussed above. Fig. 6b demonstrates the PL and PLE spectra of $Sr_{3.99}Ca(PO_4)_2SiO_4$:$0.01Eu^{2+}$. The PLE spectrum monitored at 493 nm exhibits a broad band from 260 to 450 nm, and the PL spectrum consists of a broad band centered at 493 nm under the excitation of 365 nm, which is ascribed to the electric dipole allowed the transition of the Eu^{2+} ions.[26] A notable spectral overlap between the PLE spectrum of $Sr_{3.99}Ca(PO_4)_2SiO_4$:$0.01Eu^{2+}$ and the PL spectrum of $Sr_{3.8}Ca(PO_4)_2SiO_4$:$0.1Ce^{3+}$,$0.1Na^+$ is observed. So that the energy transfer from Ce^{3+} to Eu^{2+} ions can be achieved in the $Sr_4Ca(PO_4)_2SiO_4$ system. To further confirm the possible energy transfer process, Fig. 6c illustrates the PLE and PL spectra of $Sr_{3.79}Ca(PO_4)_2SiO_4$:$0.1Ce^{3+}$,$0.1Na^+$,$0.01Eu^{2+}$ phosphors. Under the irradiation of 365 nm, the co-doped phosphor shows a broad bluish-green emission band containing the superimposed emission peaks that originated from the Eu^{2+} ions and Ce^{3+} ions. When monitoring at 493 nm and 429 nm, the two sets of PLE spectra give similar spectral profiles, which agree well with the PLE spectrum of the singly Ce^{3+} doped sample, as shown in Fig. 6a.

Fig. 5 The relationships of $\lg(x)$ versus $\lg(I/x)$. The inset shows the PL intensity of the plot of $Sr_{3.8-2x}Ca(PO_4)_2SiO_4$:$xCe^{3+}$,$xNa^+$ as a function of Ce^{3+} content.

Fig. 6 PLE (left) and PL (right) spectra of (a) $Sr_{3.8}Ca(PO_4)_2SiO_4$:$0.1Ce^{3+}$,$0.1Na^+$, (b) $Sr_{3.99}Ca(PO_4)_2SiO_4$:$0.01Eu^{2+}$, (c) $Sr_{3.79}Ca(PO_4)_2SiO_4$:$0.1Ce^{3+}$,$0.1Na^+$,$0.01Eu^{2+}$.

This journal is © The Royal Society of Chemistry 2016

J. Mater. Chem. C, 2016, **4**, 9078–9084 | 9081

Fig. 7 PL and PLE spectra of $Sr_{3.8-x}Ca(PO_4)_2SiO_4$:$0.1Ce^{3+}$,$0.1Na^+$,$xEu^{2+}$ (x = 0, 0.003, 0.01, 0.03, 0.06) phosphors.

The above comparative analysis on the PL and PLE spectra of the Ce^{3+}/Na^+ and Eu^{2+} singly doped and $Ce^{3+}/Na^+/Eu^{2+}$-co-doped $Sr_4Ca(PO_4)_2SiO_4$ phosphors proves the occurrence of the energy transfer from the Ce^{3+} to Eu^{2+} ions.[27] Therefore, the photoluminescence tuning originating from the energy transfer process can be expected.

In order to further investigate the energy transfer process between the Ce^{3+} and Eu^{2+} ions in the $Sr_4Ca(PO_4)_2SiO_4$ host, we have studied the luminescence properties of a series of samples with designed compositions. Fig. 7 displays the PL spectra of $Sr_{3.8-x}Ca(PO_4)_2SiO_4$:$0.1Ce^{3+}$,$0.1Na^+$,$xEu^{2+}$ samples under 365 nm excitation with a fixed Ce^{3+} content of 0.1 and a varying Eu^{2+} content x in the range of 0–0.06. As shown in Fig. 7, the emission peak is red-shifted from 429 nm to 493 nm with increasing concentration of Eu^{2+}. The results verified that the superimposed emission peaks originated from the Eu^{2+} ions and Ce^{3+} ions, and the observed photoluminescence tuning should be ascribed to the energy transfer from the Ce^{3+} to Eu^{2+} ions.

Normally, the energy transfer from the sensitizer to the activator may be *via* a multipolar interaction or an exchange interaction that occurs at a higher concentration. On the basis of the Dexter's energy transfer expressions of multipolar interaction, the following relation can be obtained:[28,29]

$$\frac{I_{S0}}{I_S} \propto C^{n/3} \qquad (2)$$

where I_{S0} and I_S are the luminescence intensities of the sensitizer Ce^{3+} with and without the activator Eu^{2+}; C is the concentration of the sum of Ce^{3+} and Eu^{2+}; and n = 6, 8 and 10 corresponding to dipole–dipole, dipole–quadrupole, and quadrupole–quadrupole interactions, respectively. The $I_{S0}/I_S \propto C^{n/3}$ plots are further illustrated in Fig. 8. when n = 6 we can observe a linear behavior with the optimum fitting factor of R^2 = 0.9987, indicating that energy transfer from Ce^{3+} to Eu^{2+} took place *via* the dipole–dipole mechanism.

In order to validate the energy transfer from Ce^{3+} to Eu^{2+}, we investigated the lifetime values of Ce^{3+} emission, which are calculated by analyzing decay curves of $Sr_{3.8-x}Ca(PO_4)_2SiO_4$: $0.1Ce^{3+}$,$0.1Na^+$,xEu^{2+} phosphors. Fig. 9 shows the fluorescence decay curves of Ce^{3+} emission under excitation at 354 nm and by monitoring the emission peak at 426 nm. It is found that all
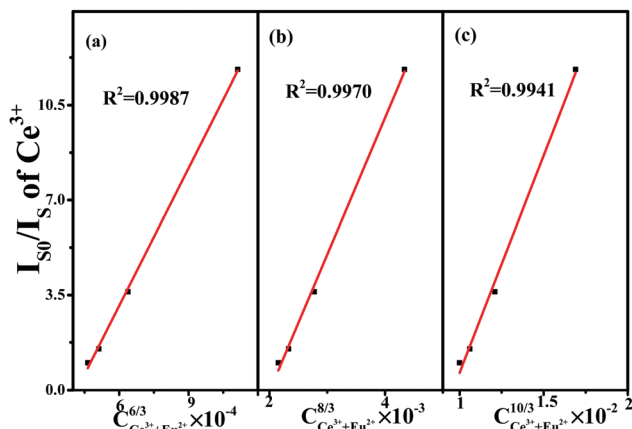

Fig. 8 Dependence of I_{S0}/I_S of Ce^{3+} on (a) $C^{6/3}$, (b) $C^{8/3}$, and (c) $C^{10/3}$.

the decay curves can be fitted well with a second-order exponential decay, which can be obtained using the equation:[30]

$$I(t) = I_0 + A_1 \exp(-t/\tau_1) + A_2 \exp(-t/\tau_2) \qquad (3)$$

where $I(t)$ is the luminescence intensity, t is the time, A_1 and A_2 are constants, and τ_1 and τ_2 are rapid and slow decay times for the exponential components, respectively. According to the parameters in eqn (3), the average lifetime τ^* can be obtained using the formula:

$$\tau^* = (A_1\tau_1^2 + A_2\tau_2^2)/(A_1\tau_1 + A_2\tau_2) \qquad (4)$$

Therefore, the decay lifetime values at 426 nm are determined to be 37.13, 32.28, 24.42, 14.42, and 9.14 ns, respectively. Obviously, the decay lifetime values decreased monotonically as the Eu^{2+} concentration increases, which also strongly demonstrated the energy transfer from Ce^{3+} to Eu^{2+}.

As shown in Fig. 10, the energy transfer efficiency (η_T) between the Ce^{3+} and Eu^{2+} ions can also be obtained from the decay lifetime values by using the following eqn (5):[31]

$$\eta_T = 1 - \frac{\tau_x}{\tau_0} \qquad (5)$$

where τ_x and τ_0 represent the lifetime values of sensitizer Ce^{3+} ions with and without the activator Eu^{2+}, respectively.
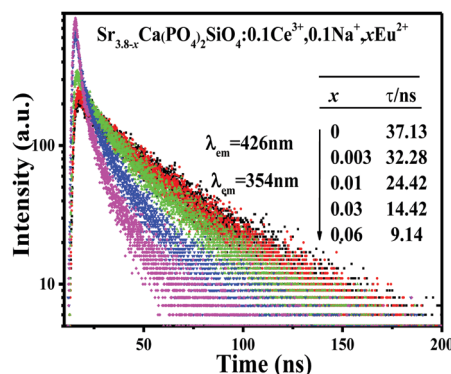
Fig. 9 Decay curves of Ce^{3+} emission in $Sr_{3.8-x}Ca(PO_4)_2SiO_4$:$0.1Ce^{3+}$, $0.1Na^+$,xEu^{2+} phosphors under excitation at 365 nm, monitored at 426 nm.

9082 | *J. Mater. Chem. C*, 2016, **4**, 9078–9084

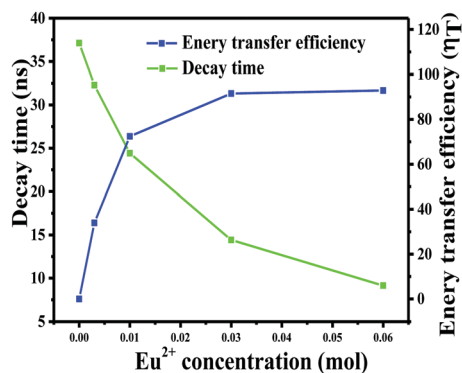This journal is © The Royal Society of Chemistry 2016

Fig. 10 Dependence of the fluorescence lifetime of the Ce^{3+} and energy transfer efficiency on the doped Eu^{2+} molar concentration in $Sr_{3.8-x}Ca(PO_4)_2SiO_4$:$0.1Ce^{3+},0.1Na^+,xEu^{2+}$ samples.

Fig. 12 CIE chromaticity diagram and a series of digital photographs of the selected $Sr_{3.8-x}Ca(PO_4)_2SiO_4$:$0.1Ce^{3+},0.1Na^+,xEu^{2+}$ (x = 0, 0.003, 0.01, 0.03 and 0.06) phosphors (λ_{ex} = 365 nm).

With increasing Eu^{2+} concentration the energy transfer efficiencies increase gradually and η_T values are calculated to be 13.06%, 34.23%, 61.16% and 75.38% for the $Sr_{3.8-x}Ca(PO_4)_2SiO_4$:$0.1Ce^{3+},0.1Na^+,xEu^{2+}$ phosphors with different Eu^{2+} concentrations of x = 0.003, 0.01, 0.03 and 0.06.

3.4 Thermal quenching and photoluminescence tuning of $Sr_4Ca(PO_4)_2SiO_4$:Ce^{3+},Na^+,Eu^{2+} phosphors

Fig. 11a typically presents the temperature dependent emission spectra of $Sr_{3.79}Ca(PO_4)_2SiO_4$:$0.1Ce^{3+},0.1Na^+,0.01Eu^{2+}$ phosphors upon 365 nm excitation in the range of 25–300 °C, and it is found that emission intensities decrease and the emission peaks shift to the blue region with increasing temperature. By normalizing the initial luminescence intensity to 1.0, the relative emission intensities of the Ce^{3+}/Na^+ or Eu^{2+} singly doped and $Ce^{3+}/Na^+/Eu^{2+}$-co-doped $Sr_4Ca(PO_4)_2SiO_4$ phosphors as a function of

Fig. 11 (a) PL spectra (λ_{ex} = 365 nm) of the selected $Sr_{3.79}Ca(PO_4)_2SiO_4$:$0.1Ce^{3+},0.1Na^+,0.01Eu^{2+}$ phosphor at different temperatures in the range of 25–300 °C. (b) The relative emission intensities as a function of temperature for typical $Ce^{3+}/Na^+,Eu^{2+}$ singly doped and $Ce^{3+}/Na^+,Eu^{2+}$-co-doped $Sr_4Ca(PO_4)_2SiO_4$ phosphors.

temperature are displayed in Fig. 11b, which shows that the relative PL intensity slowly decreases with increasing temperature. When the temperature was increased to 150 °C, the PL intensity of the sample drops to 71.3%, 70.1% and 66.0% of the initial value at room temperature for the corresponding compositions of $Sr_{3.79}Ca(PO_4)_2SiO_4$:$0.1Ce^{3+},0.1Na^+,0.01Eu^{2+}$, $Sr_{3.99}Ca(PO_4)_2SiO_4$:$0.01Eu^{2+}$ and $Sr_{3.8}Ca(PO_4)_2SiO_4$:$0.1Ce^{3+},0.1Na^+$ phosphors. The better thermal quenching luminescence behavior will be useful for the high temperature and high power application when this kind of phosphor is used as the blue-green components in UV-pumped WLEDs.

Fig. 12 shows the chromaticity coordinates of the as-reported $Sr_{3.8-x}Ca(PO_4)_2SiO_4$:$0.1Ce^{3+},0.1Na^+,xEu^{2+}$ phosphors on the Commission Internationale de l'Eclairage (CIE) chromaticity diagram. The CIE chromaticity coordinates for different samples in $Sr_{3.8-x}Ca(PO_4)_2SiO_4$:$0.1Ce^{3+},0.1Na^+,xEu^{2+}$ phosphors were measured based on the corresponding PL spectra upon 365 nm excitation. As shown in Fig. 12, we can clearly see that the emission colors of the phosphors can be easily modulated from blue to green by simply changing the value of x from 0 to 0.06. Accordingly, the corresponding CIE coordinates change from (0.156, 0.0717) to (0.233, 0.346), due to the variation of the emission composition of the Ce^{3+} and Eu^{2+} ions. The inset in Fig. 12 illustrates the digital photos of this series of phosphors under 365 nm UV lamp excitation. These results indicate that the as-reported and composition-optimized phosphor might act as a potential candidate for blue-green components in UV-pumped WLEDs.

4. Conclusion

A new apatite-type phase that originated from the substitution of a Sr cation by a Ca cation in the $Sr_5(PO_4)_2(SiO_4)$ has been prepared with the nominal chemical composition of $Sr_4Ca(PO_4)_2(SiO_4)$. The crystal structure of $Sr_4Ca(PO_4)_2(SiO_4)$ has been analysed by the difference electron map, and further resolved by the Rietveld refinement, and the final composition has been determined as $Sr_4Ca(PO_4)_{(2+x)}(SiO_4)_{(1-x)}(OH)_x$ (x = 0.64), which crystallized in the hexagonal cell (space group $P6_3/m$) with

This journal is © The Royal Society of Chemistry 2016

J. Mater. Chem. C, 2016, **4**, 9078–9084 | 9083

lattice constants $a = b = 9.67202$ (8), $c = 7.25393$ (7), $V = 587.68$ (1), $Z = 2$. The photoluminescence properties of Ce^{3+}/Na^+ or Eu^{2+} singly doped and $Ce^{3+}/Na^+/Eu^{2+}$-co-doped $Sr_4Ca(PO_4)_2SiO_4$ phosphors have been investigated in detail. When Ce^{3+} and Eu^{2+} were codoped in $Sr_4Ca(PO_4)_2SiO_4$, the photoluminescence spectra displayed tunable blue-green emission by varying their relative concentrations. The effective energy transfer from the Ce^{3+} to Eu^{2+} has been discussed and verified based on the measured spectra and the decay curves, and the dipole–dipole interaction mechanism should be mainly responsible for the energy transfer process. The as-developed $Sr_4Ca(PO_4)_2SiO_4$: Ce^{3+},Na^+,Eu^{2+} phosphor might act as a potential candidate for blue-green components in UV-pumped WLEDs.

Acknowledgements

Notes and references

1 D. Mazza, M. Tribaudino, A. Delmastro and B. Lebech, *J. Solid State Chem.*, 2000, **155**, 389–393.

2 T. Baikie, G. M. H. Ng, S. Madhavi, S. S. Pramana, K. Blake, M. Elcombe and T. J. White, *Dalton Trans.*, 2009, 6722–6726.

3 Y. Tian, Y. Wei, Y. Zhao, Z. Quan, G. Li and J. Lin, *J. Mater. Chem. C*, 2016, **4**, 1281–1294.

4 M. Schumacher and M. Gelinsky, *J. Mater. Chem. B*, 2015, **3**, 4626–4640.

5 P. K. Pandis, E. Xenogiannopoulou, P. M. Sakkas, G. Sourkouni, C. Argirusis and V. N. Stathopoulos, *RSC Adv.*, 2016, **6**, 49429–49435.

6 M. Jiao, Y. Jia, W. Lu, W. Lv, Q. Zhao, B. Shao and H. You, *J. Mater. Chem. C*, 2014, **2**, 90–97.

7 Z. Xia, C. Ma, M. S. Molokeev, Q. Liu, K. Rickert and K. R. Poeppelmeier, *J. Am. Chem. Soc.*, 2015, **137**, 12494–12497.

8 Z. Xia, S. Miao, M. S. Molokeev, M. Chen and Q. Liu, *J. Mater. Chem. C*, 2016, **4**, 1336–1344.

9 T. Wang, Q. Xiang, Z. Xia, J. Chen and Q. Liu, *Inorg. Chem.*, 2016, **55**, 2929–2933.

10 B. Dickens and W. E. Brown, *Tschermaks Mineral. Petrogr. Mitt.*, 1971, **16**, 1–27.

11 M. Y. Chen, Z. G. Xia, M. S. Molokeev and Q. L. Liu, *Inorg. Chem.*, 2015, **54**, 11369–11376.

12 H. P. Ji, Z. H. Huang, Z. G. Xia, M. S. Molokeev, V. V. Atuchin, M. H. Fang and S. F. Huang, *Inorg. Chem.*, 2014, **53**, 5129–5135.

13 S. Miao, Z. Xia, M. S. Molokeev, M. Chen, J. Zhang and Q. Liu, *J. Mater. Chem. C*, 2015, **3**, 4616–4622.

14 M. Shang, C. Li and J. Lin, *Chem. Soc. Rev.*, 2014, **43**, 1372–1386.

15 G. Blasse and A. Bril, *Phys. Lett. A*, 1969, **28**, 572–573.

16 J. Gan, Y. Huang, L. Shi, X. Qiao and H. J. Seo, *Mater. Lett.*, 2009, **63**, 2160–2162.

17 H.-S. Roh, S. Hur, H. J. Song, I. J. Park, D. K. Yim, D.-W. Kim and K. S. Hong, *Mater. Lett.*, 2012, **70**, 37–39.

18 Y. Huang, J. Gan, R. Zhu, X. Wang and H. J. Seo, *J. Electrochem. Soc.*, 2011, **158**, J334–J340.

19 S. Xin, Y. Wang, G. Zhu, F. Zhang, Y. Gong, Y. Wen and B. Liu, *Mater. Res. Bull.*, 2013, **48**, 1627–1631.

20 D. Geng, M. Shang, Y. Zhang, H. Lian, Z. Cheng and J. Lin, *J. Mater. Chem. C*, 2013, **1**, 2345–2353.

21 K. Sudarsanan and R. A. Young, *Acta Crystallogr., Sect. B: Struct. Crystallogr. Cryst. Chem.*, 1972, **28**, 3668–3670.

22 Z. Xia, M. S. Molokeev, W. B. Im, S. Unithrattil and Q. Liu, *J. Phys. Chem. C*, 2015, **119**, 9488–9495.

23 L. G. Van Uitert, *J. Electrochem. Soc.*, 1967, **114**, 1048–1053.

24 H. Y. Xiao, Z. G. Xia, L. B. Liao, J. Zhou and J. Q. Zhuang, *J. Alloys Compd.*, 2012, **534**, 97–100.

25 Z. G. Xia, Y. Y. Zhang, M. S. Molokeev and V. V. Atuchin, *J. Phys. Chem. C*, 2013, **117**, 20847–20854.

26 X. Chen, Z. G. Xia and Q. L. Liu, *Dalton Trans.*, 2014, **43**, 13370–13376.

27 M. M. Shang, G. G. Li, D. L. Geng, D. M. Yang, X. J. Kang, Y. Zhang, H. Z. Lian and J. Lin, *J. Phys. Chem. C*, 2012, **116**, 10222–10231.

28 D. L. Dexter, *J. Chem. Phys.*, 1953, **21**, 836–850.

29 D. L. Dexter and J. H. Schulman, *J. Chem. Phys.*, 1954, **22**, 1063–1070.

30 M. Chen, Z. Xia, M. S. Molokeev and Q. Liu, *J. Mater. Chem. C*, 2015, **3**, 12477–12483.

31 S. Miao, Z. Xia, M. S. Molokeev, J. Zhang and Q. Liu, *J. Mater. Chem. C*, 2015, **3**, 8322–8328.

9084 | *J. Mater. Chem. C*, 2016, **4**, 9078–9084

This journal is © The Royal Society of Chemistry 2016